Optics and Lasers in Engineering 51 (2013) 790–795

Contents lists available at SciVerse ScienceDirect

Optics and Lasers in Engineering

journal homepage: www.elsevier.com/locate/optlaseng

Phase-optimized dithering technique for high-quality 3D shape measurement

Junfei Dai [a], Song Zhang [b,*]

[a] Mathematics Department, Zhejiang University, Zhejiang 310027, China
[b] Mechanical Engineering Department, Iowa State University, Ames, IA 50011, United States

ARTICLE INFO

Article history:
Received 10 December 2012
Received in revised form
19 January 2013
Accepted 2 February 2013
Available online 20 February 2013

Keywords:
Fringe analysis
3D shape measurement
Dithering

ABSTRACT

Our recent study showed that the Bayer-dithering technique could substantially improve 3D measurement quality for the binary defocusing method. Yet, the dithering technique was developed to optimize the appearance or intensity representation, rather than the phase, of an image. This paper presents a framework to optimize the Bayer-dithering technique in phase domain by iteratively mutating the status (0 or 1) of a binary pixel. We will demonstrate that the proposed optimization technique can drastically reduce the phase error when the projector is nearly focused.

1. Introduction

Digital fringe projection (DFP) techniques have been increasing used for high-quality 3D shape measurement due to its flexibility [1]. However, it is still challenging to simultaneously achieve both high measurement speed and high accuracy. The conventional DFP system utilizes a computer to generate sinusoidal fringe patterns that are further sent to the projector; and since it usually requires 8 bits to represent a sinusoidal pattern, the measurement speed is typically limited to 120 Hz (typical video projector refresh rate) [2]. Moreover, to cope with human vision, most commercially available video projectors are nonlinear (i.e., linear intensity inputs produce nonlinear intensity outputs); and this will introduce measurement error if the projector nonlinearity is not compensated [3].

To address the challenges of the conventional DFP technique, we recently developed the binary defocusing technique [4], which has successfully made speed breakthroughs [5]. However, the binary defocusing technique cannot achieve the same measurement capability as the conventional DFP methods: (1) the measurement accuracy is lower due to the high-frequency harmonics influences and (2) the measurement range is smaller since the projector must be properly defocused for high-quality measurement, leaving the large room of nearly focused regime unusable [6].

Lately, substantial improvements have been made through borrowing the pulse width modulation (PWM) techniques developed in power electronics to this field [7,8]. The PWM technique essentially modulates the binary pattern such that the high frequency harmonics can be easier to be suppressed, or eliminated, after defocusing. They all achieved better measurement quality, but have limited improvements when fringe stripes are wide [9]. The PWM technique is, after all, one-dimensional optimization in nature, and thus cannot completely take advantages of the binary defocusing technique since the fringe pattern is two-dimensional.

Modulating the binary patterns in both x and y dimensions could further improve the binary defocusing technique. Xian and Su proposed an area modulation technique that could generate high-quality fringe patterns by highly precisely micro-machined gratings [10]. However, it is difficult to adopt such a technique in a DFP system since it requires a lot more and smaller pixels than a digital video projector can provide. We recently proposed a technique to locally modulate the pixels so that a squared binary pattern emulate a triangular pattern when the projector is nearly focused [11]. Since the high-frequency harmonic influences of a triangular wave drop more rapidly, it is easier to generate an ideal sinusoidal pattern through defocusing. Yet, similar to PWM techniques, this technique has problem when the desired fringe stripes are wide.

It turned out that, since 1960s [12], representing grayscale images with binary images has been extensively studied in the fields of image processing and printing: this technique is called haftoning or dithering. Over the past many years, various dithering techniques have been developed that include random dithering [13], ordered dithering [14], and error diffusion [15] techniques. Our recent study [16] showed that for a binary defocusing technique, the Bayer-dithering method could substantially improve the measurement

* Corresponding author. Tel.: +1 515 294 0723; fax: +1 515 294 3261.
E-mail addresses: isusong@gmail.com, song@iastate.edu (S. Zhang).

0143-8166/$ - see front matter © 2013 Elsevier Ltd. All rights reserved.
http://dx.doi.org/10.1016/j.optlaseng.2013.02.003

quality even when the fringe stripes are very wide. The dithering techniques, after all, were developed to optimize the appearance or intensity, rather than the phase, of an image. However, for 3D shape measurement, the phase quality determines the measurement quality, and thus it is more important to generate high-quality phase than appearance [9].

This paper presents a framework to further improve the Bayer-dithering technique by optimizing the dithered patterns in the phase domain instead of the intensity domain. Specifically, by iteratively mutating the status (0 or 1) of a binary pixel, the proposed optimization technique minimizes the resultant overall phase error comparing with the ideal phase. By this means, the phase-optimized dithering technique can substantially improve the binary dithering technique, making it closer to the conventional DFP technique. Both simulations and experiments will be presented to show that the proposed technique can drastically reduce the phase error when the projector is nearly focused.

Section 2 explains the principle of the phase-shifting algorithm and the dithering technique. Section 3 presents the proposed framework for phase optimization. Section 4 shows simulation results. Section 5 presents the experimental results, and finally Section 6 summarizes this paper.

2. Principle

2.1. Three-step phase-shifting algorithm

A simple three-step phase-shifting algorithm with a phase shift of $2\pi/3$ was used to test the generated pattern. Three fringe images can be described as

$$I_1(x,y) = I'(x,y) + I''(x,y)\cos[\phi - 2\pi/3], \tag{1}$$

$$I_2(x,y) = I'(x,y) + I''(x,y)\cos[\phi], \tag{2}$$

$$I_3(x,y) = I'(x,y) + I''(x,y)\cos[\phi + 2\pi/3], \tag{3}$$

where $I'(x,y)$ is the average intensity, $I''(x,y)$ is the intensity modulation, and $\phi(x,y)$ is the phase to be solved for

$$\phi(x,y) = \tan^{-1}\frac{\sqrt{3}(I_1 - I_3)}{2I_2 - I_1 - I_3}. \tag{4}$$

This equation provides the phase ranging $[-\pi, +\pi)$ with 2π discontinuities. A continuous phase map can be obtained by adopting a spatial or temporal phase unwrapping algorithm. In this research, we used the temporal phase unwrapping framework introduced in [17].

2.2. Bayer-dithering technique

Dithering is a technique used in computer graphics to create the illusion of color depth in images with a limited color quantization. To approximate a sinusoidal pattern with a binary pattern, various dithering techniques can be used, such as the simple thresholding, the random dithering, the ordered dithering (e.g., the Bayer-ordered dithering). Among these dithering methods, the ordered dithering technique has been extensively used due to its simplicity and its potential for parallel processing. The Bayer-dithering technique compares the original image with a 2-D fixed block called Bayer kernel: if the grayscale value is larger, the pixel turned to 1 (or 255 grayscale value), otherwise to 0. Among the kernels used, Bayer has shown that if the sizes of the matrices are 2^N (N is an integer), there is an optimal dither pattern that results in the pattern noise being as high-frequency as possible [14]. By doing so, the dithered image can be very close to the original image since the high-frequency noises can be effectively reduced by applying a low-pass filter. The Bayer kernels can be obtained as follows:

$$M_1 = \begin{bmatrix} 0 & 2 \\ 3 & 1 \end{bmatrix}, \tag{5}$$

which is the smallest 2×2 base. Larger Bayer patterns can be generated with smaller patterns using the following equation:

$$M_{n+1} = \begin{bmatrix} 4M_n & 4M_n + 2U_n \\ 4M_n + 3U_n & 4M_n + U_n \end{bmatrix}, \tag{6}$$

where U_n is n-dimensional unit matrix (all elements are 1). In this research, we found that the 16×16 Bayer kernel produces the best results for all tested fringe stripes, and thus is utilized.

3. Optimization framework

We developed an optimization framework named *phase-optimized dithering technique* to reduce the overall phase error. During optimization process, *improvement rule* and *convergence rule* were defined for this framework. The improvement rule guides the algorithm to make the decision on whether the status (0 or 1) of a dithered pixel should be mutated (from 0 to 1 or from 1 to 0). The convergence rule tells the algorithm when it should stop its iterations.

This optimization framework can be divided into the following major steps:

- *Step*1*: Error pixel detection.* Utilizing a three-step phase-shifting on ideal sinusoidal phase-shifted fringe patterns, we can obtain the ideal phase $\Phi(x,y)^i$. We can also obtain the $\Phi^d(x,y)$ from the dithered patterns after applying a small Gaussian filter (i.e., filter size of 5×5 and standard deviation of 5/3 pixels, which is the same for the rest of the paper unless it is otherwise specified) to emulate the nearly focused projector. For a given pixel (i,j), if its phase error $\Delta_\Phi(i,j) = |\Phi(x,y)^i - \Phi^d(x,y)| > \epsilon$, this pixel is marked

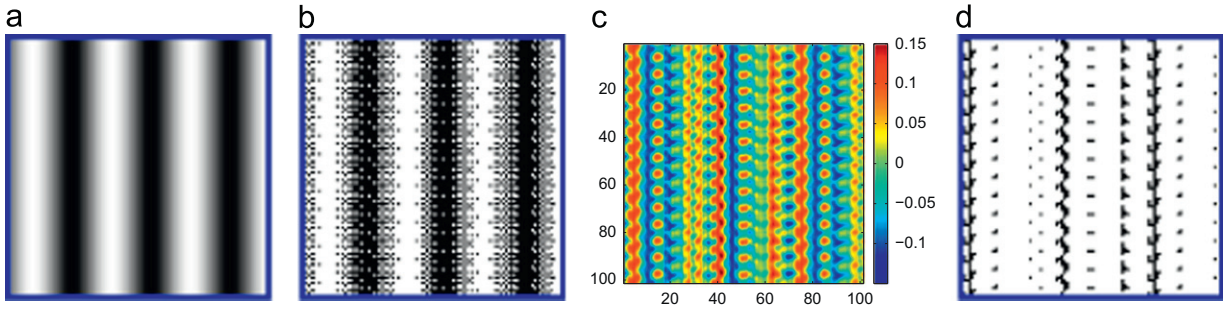

Fig. 1. Error pixel detection example. (a) One of ideal sinusoidal fringe patterns. (b) Bayer-dithered pattern. (c) Phase difference map Δ_Φ. (d) Error pixel map (black pixels) when $\epsilon = 0.10$ rad.

as the error pixel. Here, ϵ is a small predefined threshold. All error pixels are combined to form an error pixel map E_m, which was stored for further processing. Fig. 1 shows an example. Fig. 1(a)–(c) respectively shows the sinusoidal pattern, the Bayer-dithered pattern, and the phase difference map. If a threshold of $\epsilon = 0.10$ rad was chosen, the error pixels can be identified, as shown in Fig. 1(d). In the error pixel map, the black pixels are those who need to be further processed through optimization.

- *Step2: Error pixel mutation*. For each error pixel, its binary status is altered to the other value (i.e., 1 to 0 or 0 to 1); and the difference phase map Δ_Φ is computed. Comparing the phase root-mean-square (rms) error (σ^a) of the Δ_Φ after the pixel mutation and that (σ^b) before its mutation, if $\sigma^a > \sigma^b$, the mutation should not occur since it deteriorate the fringe quality. This is the *improvement rule* that indicates that whether the phase quality improves or not after mutation.
- *Step3: Iterations*. The fact is that if the status of an error pixel is alternated, it will affect its neighboring pixels due to the usage of a 5×5 Gaussian filter for phase error determination. Therefore, after completing the whole image, the algorithm will to back to Step 2 again for optimization until the optimization converges using the *convergence rule*. The convergence rule we used here is that the improvement of phase rms error for a round of processing is less than 0.01%.
- *Step4: Threshold reduction*. Once Step 3 is complete (i.e., the algorithm converges), we reduce the threshold and go back to Step 1 for another iteration. We found that for all tests we tried, the phase error becomes very small after approximately 15 rounds of iterations. Fig. 2 shows an example when the fringe pitch (number of pixels per fringe period) is 60, the phase rms errors after each iteration, where 0 iteration means the original Bayer-dithered patterns.

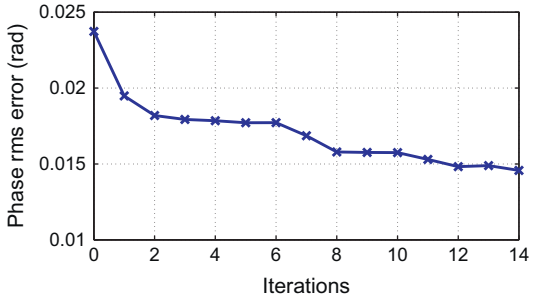

Fig. 2. The phase rms errors after each round of optimization with reduced thresholds.

4. Simulations

It can be seen that the proposed framework is to optimize the dithered patterns in the phase domain instead of the intensity domain. Specifically, by iteratively alternating the status (0 or 1) of an error dithered pixel, the proposed optimization technique minimizes the resultant overall phase error comparing with the ideal phase. By this means, the phase-optimized dithering technique can substantially improve the binary dithering technique, making it closer to conventional DFP technique while only binary instead of 8-bit structured patterns are required. Fig. 3 shows optimized pattern after 15 iterations for the dithered pattern illustrated in Fig. 1(b). Fig. 3(b) shows the error map. Comparing with the error map using the original Bayer-dithered pattern shown in Fig. 1(c), the error is substantially smaller after applying the proposed optimization framework. Quantitatively, the phase rms error was reduced from 0.068 to 0.025 rad.

The proposed optimization framework was verified through simulations. We firstly simulated fringe patterns with a wide range of fringe stripe breadths. In this simulation, we used fringe pitches, number of pixels per fringe period, of 18, 30, 60, 120, 240, 480, 600, to generate fringe patterns whose resolution is 800×600. These selections represent both dense fringe patterns and wide fringe patterns for a DFP system. After applying a 5×5 Gaussian filter, the phase error was determined for each pixel. Fig. 4 compares the phase rms errors before and after optimization for 15 rounds of iterations. Fig. 4(a) shows the absolute phase rms errors. One may notice that the phase errors for the smaller fringe pitches are larger. This appears unreasonable as we all know that narrower fringe patterns shall give smaller *phase errors*. Yet, we may ignore the fact that the errors typically refer to relative error (in percentage). To show that the narrower fringe patterns actually generate better phase, we plotted the relative phase error percent, as shown in Fig. 4(b). This figure shows that narrower fringe patterns indeed offer better phase quality. These experiments clearly showed that the phase errors were drastically reduced with the proposed optimization technique.

We also simulated a more complex 3D shape, as shown in Fig. 5(a). The depth profile is quite complex. The depth map can then be encoded three phase-shifted fringe patterns shown in Fig. 5(b)–(d). These patterns contain fringes varying from dense to sparse, which are representative for captured fringe patterns if the geometric shape is complex.

These sinusoidal fringe patterns were dithered into binary patterns using the Bayer-dithering technique; and the optimized with the proposed optimization framework. Fig. 6 shows the comparing results. The Bayer-dithered pattern for Fig. 5(b) is shown

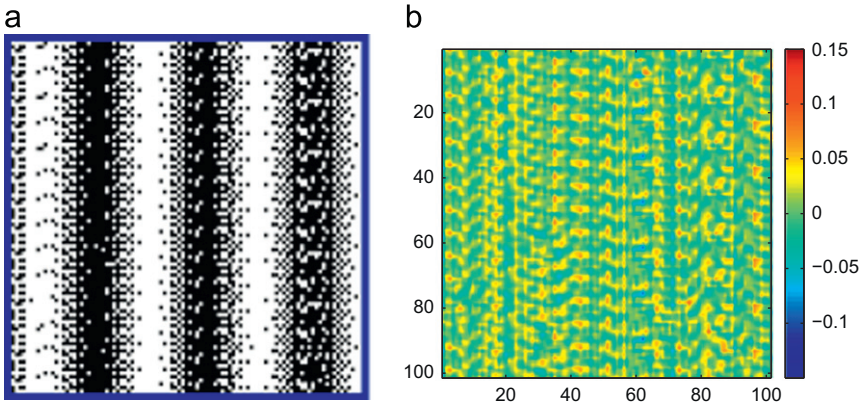

Fig. 3. Comparing the optimized results and the dithered results. (a) The optimized pattern for the dithered pattern shown in Fig. 1(b). (b) The phase difference map Δ_Φ.

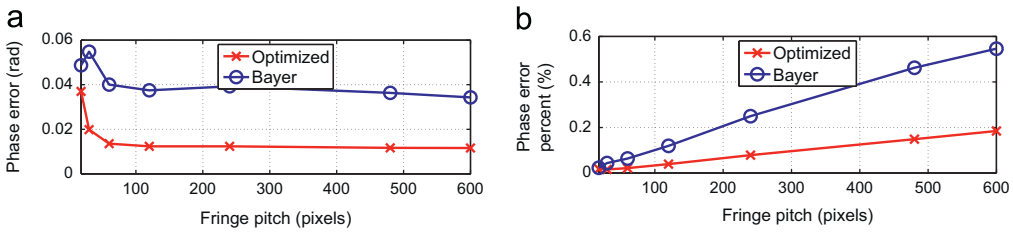

Fig. 4. Comparison of the dithering technique and the optimized dithering technique. (a) Absolute phase rms error. (b) Relative phase rms error in percentage.

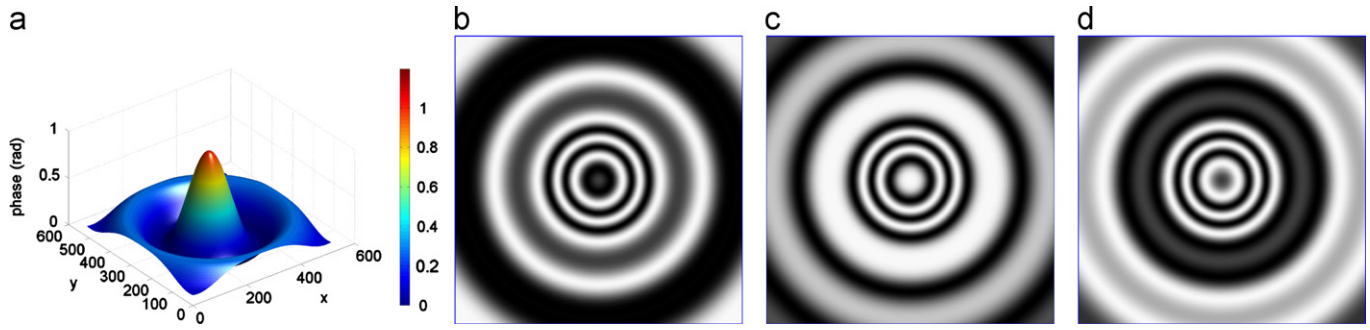

Fig. 5. Example of more complex 3D shape. (a) Represented 3D profile. (b)–(d) Three phase-shifted fringe patterns.

in Fig. 6(a). Applying a 5×5 Gaussian filter, we recovered the depth profile from the dithered patterns, as shown in Fig. 6(b). We then applied the optimization framework to the dithered fringe patterns, and recovered the 3D profile from the optimized patterns after applying a 5×5 Gaussian filter. Fig. 6(d) and (e) respectively shows the optimized dithered pattern after 15 iterations and the reconstructed 3D profile. The difference between the recovered 3D profiles and the ideal one was plotted in Fig. 6(b) and (e). The improvement was, once again, substantial: the phase rms error was reduced from 0.055 to 0.035 rad.

5. Experiments

We also carried out experiments to verify the performance of the proposed optimization framework. We utilized a previously developed 3D shape measurement to perform all the experiments. The hardware system includes a digital-light-processing (DLP) projector (Model: Samsung SP-P310MEMX) and a charge-coupled-device (CCD) camera (Model: Jai Pulnix TM-6740CL). The camera was attached with a 16 mm focal length Mega-pixel lens (Model: Computar M1614-MP) with F/1.4 to 16C. We chose the camera resolution of 640×480 for all the experiments. The projector has a native resolution of 800×600 with a projection distance of 0.49–2.80 m.

The first sequence of experiments were to measure a uniform flat board with the Bayer-dithered patterns, and the optimized-dithered patterns. From each set of fringe patterns, the phase can be unwrapped and compared against the ideal phase Φ^i. In this research, the ideal phase was obtained by a nine-step phase-shifting algorithm with a fringe pitch of 18. All the phase errors are compared against this ideal phase map. During all experiments, the projector and the camera remain untouched to ensure that they operate under exactly the same condition.

Fig. 7 shows comparing results for different fringe pitches with the Bayer-dithered patterns, and the optimized patterns. Fig. 7(a) shows one of the captured fringe patterns for the fringe pitch of 60 pixels. For this experiment, the projector was nearly focused as the binary structures are clearly seen on this image. Fig. 7(b) and (c) shows the errors for different fringe pitches. For all fringe pitches, the phase errors from the optimized dithered patterns were always drastically smaller than those from the Bayer-dithered patterns. These experiments indicated that the optimized dithering technique indeed substantially improved the phase quality when the projector is nearly focused.

Further analysis was made under this measurement condition to better illustrate the differences between these measurement conditions. Fig. 8 shows the results when the fringe pitch is 18. For all our analysis, we minimized the random noise influence by the reference plane by smoothing the reference phase with a large Gaussian filter (size of 11×11). Fig. 8(a) shows one cross section of the reference plane after removing gross slope. It clearly shows the reference plane is very smooth without visible random noises. Fig. 8(b) shows the cross sections of the phase error maps for the Bayer-dithered patterns and the optimized patterns. Again, this figure clearly showed improvements using the proposed optimized patterns.

We also measured a more complex 3D shape, David Head, to further experimentally verify the proposed technique. Fig. 9 shows the results. Fig. 9(a) shows the photograph of the captured sculpture. We firstly measured such a complex 3D shape with a conventional DFP method whose result is shown in Fig. 9(d). The same 3D sculpture was then measured with the Bayer-dithered patterns as well as the proposed optimized-dithered patterns under the exactly the same settings. Fig. 9(b) shows one of the Bayer-dithered patterns and Fig. 9(e) shows the recovered 3D shape. It clearly showed the improvement of the proposed method over the conventional Bayer-dithering technique.

6. Conclusion

This paper has presented an optimization framework to improve the phase quality for the Bayer-dithered pattern. We found that when the projector is nearly focused, this optimization framework

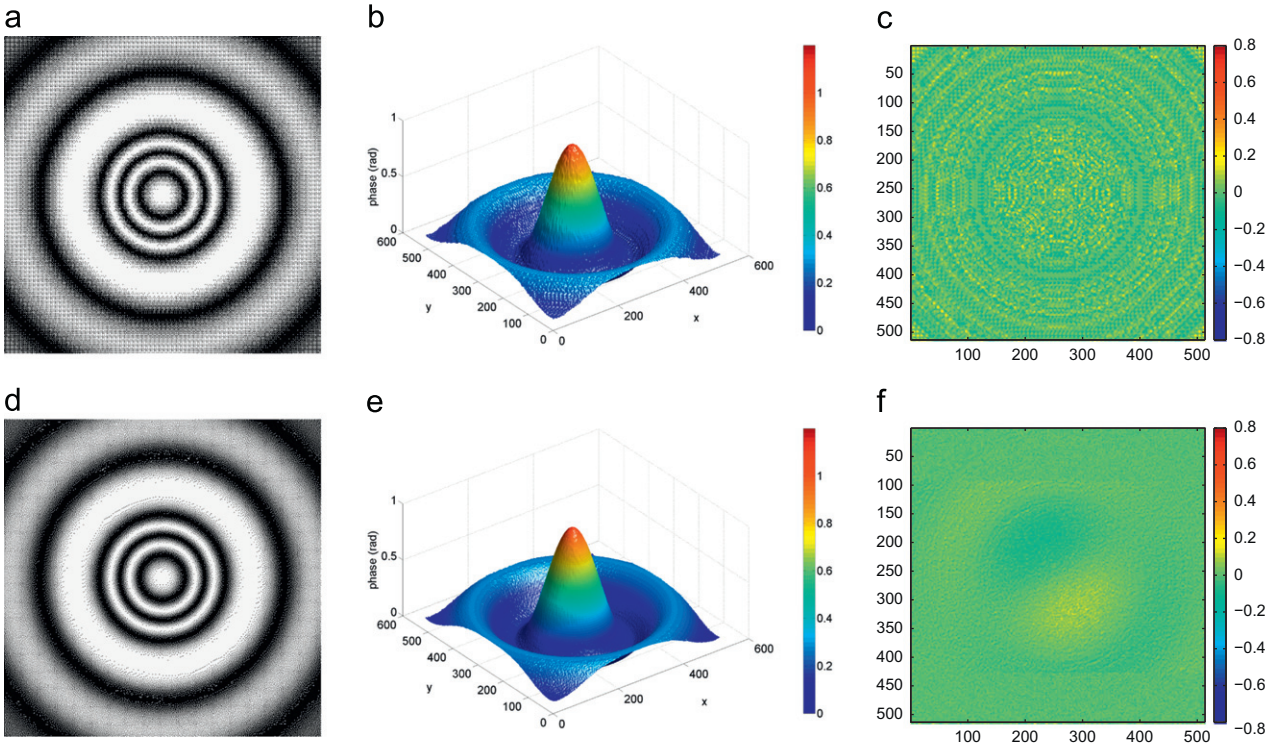

Fig. 6. Results for the example shown in Fig. 5. (a)–(c) One of the Bayer-dithered patterns; 3D reconstructed result, and the depth error map. (d)–(e) One of the optimized dithered patterns, 3D reconstructed result and the depth error.

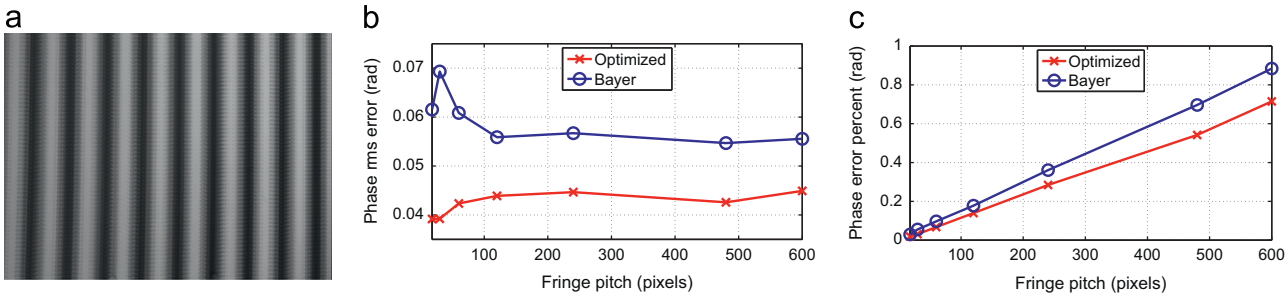

Fig. 7. Experimental validation for different fringe pitches. (a) One of the captured fringe patterns. (b) Absolute phase rms errors. (c) Relative phase rms errors.

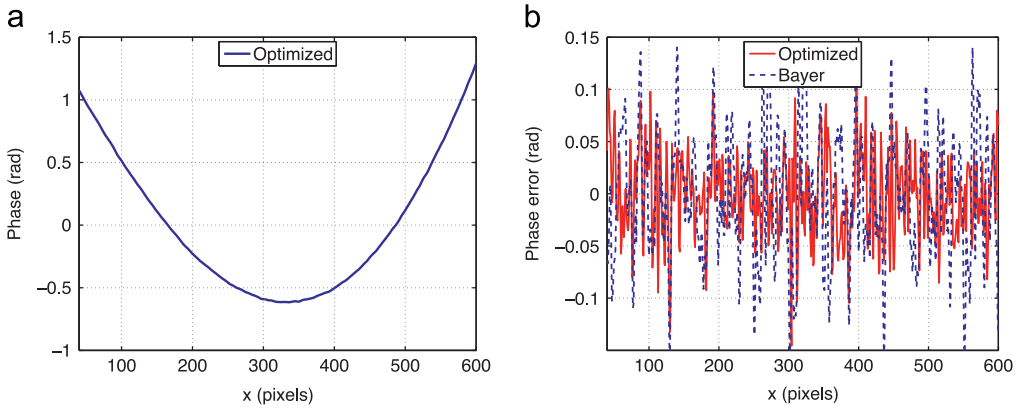

Fig. 8. Comparison of flat board measurements. (a) Cross section of the reference plane after removing the gross slope. (b) Cross sections of the phase error maps.

could substantially reduce the phase error, and thus enhance the measurement quality. Both simulation and experimental results demonstrated the success of the proposed technique. One should note that even though only ordered-Bayer-dithering technique was tested, we also found that the proposed technique could also be used to improve the more complex error-diffusion technique, albeit

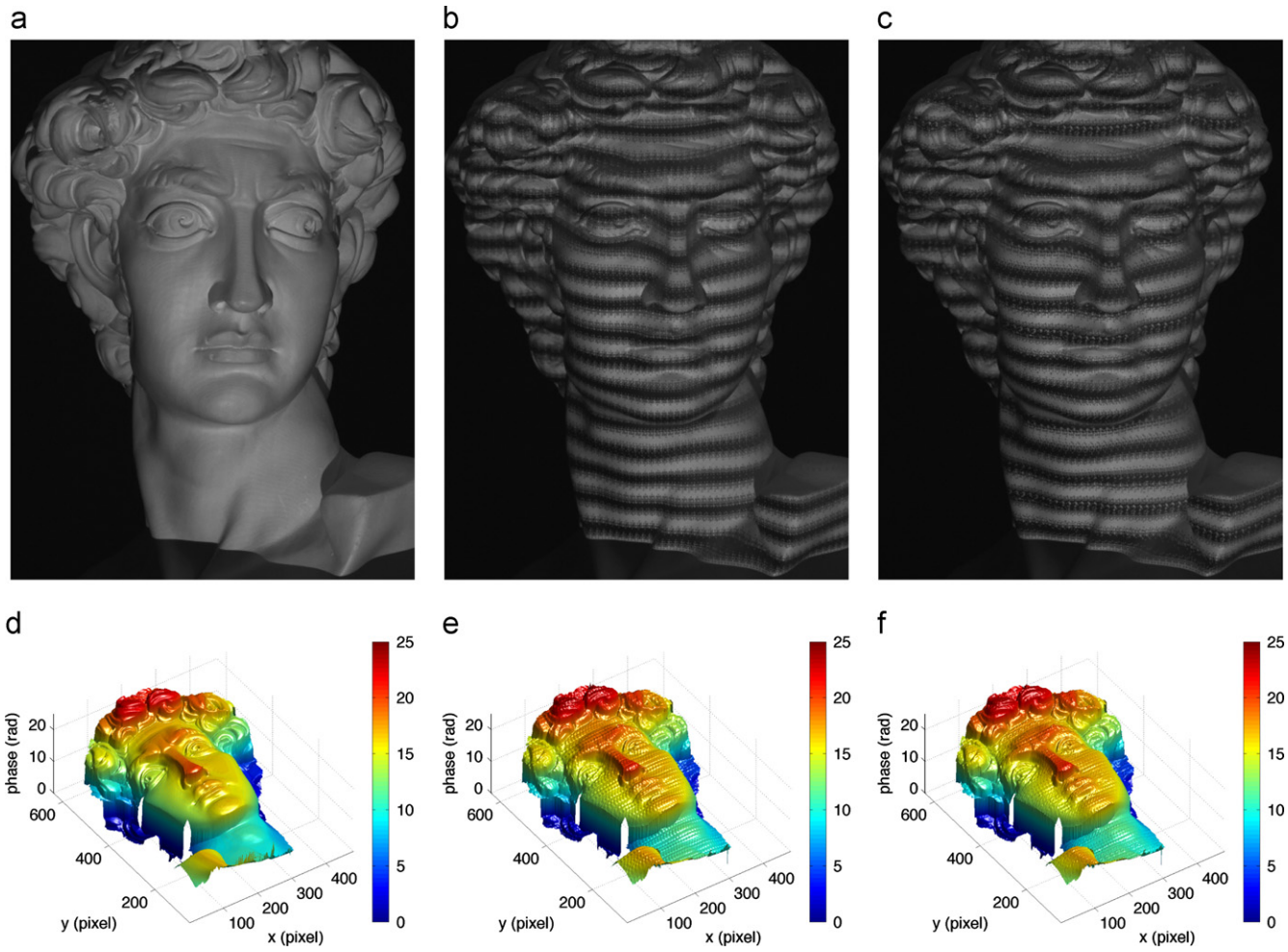

Fig. 9. Measurement results of the David Head. (a) Photograph. (b) One Bayer-dithered pattern. (c) One optimized-dithered pattern. (d) Recovered 3D shape with the conventional DFP method. (e) Recovered 3D shape with Bayer-dithered patterns. (f) Recovered 3D shape with optimized-dithered patterns.

the enhancement was not as significant. This is because the error-diffusion technique has already provided better phase quality than the Bayer-dithering technique.

Acknowledgments

This research was partially supported by the National Science Foundation under the Project number of CMMI-1150711.

References

[1] Geng G. Structured-light 3D surface imaging: a tutorial. Adv Opt Photonics 2011;3(2):128–60.
[2] Zhang S. Recent progresses on real-time 3-D shape measurement using digital fringe projection techniques. Opt Laser Eng 2010;48(2):149–58.
[3] Lei S, Zhang S. Digital sinusoidal fringe generation: defocusing binary patterns vs focusing sinusoidal patterns. Opt Laser Eng 2010;48(5):561–9.
[4] Lei S, Zhang S. Flexible 3-D shape measurement using projector defocusing. Opt Lett 2009;34(20):3080–2.
[5] Zhang S, van der Weide D, Oliver J. Superfast phase-shifting method for 3-D shape measurement. Opt Express 2010;18(9):9684–9.
[6] Xu Y, Ekstrand L, Dai J, Zhang S. Phase error compensation for three-dimensional shape measurement with projector defocusing. Appl Opt 2011;50(17):2572–81.
[7] Ajubi GA, Ayubi JA, Martino JMD, Ferrari JA. Pulse-width modulation in defocused 3-D fringe projection. Opt Lett 2010;35:3682–4.
[8] Wang Y, Zhang S. Optimum pulse width modulation for sinusoidal fringe generation with projector defocusing. Opt Lett 2010;35(24):4121–3.
[9] Wang Y, Zhang S. Comparison among square binary, sinusoidal pulse width modulation and optimal pulse width modulation, methods for three-dimensional shape measurement. Appl Opt 2012;51(7):861–72.
[10] Xian T, Su X. Area modulation grating for sinusoidal structure illumination on phase-measuring profilometry. Appl Opt 2001;40(8):1201–6.
[11] Lohry W, Zhang S. 3D shape measurement with 2D area modulated binary patterns. Opt Laser Eng 2012;50(7):917–21.
[12] Schuchman TL. Dither signals and their effect on quantization noise. IEEE Trans Commun Technol 1964;12(4):162–5.
[13] Purgathofer W, Tobler R, Geiler M. Forced random dithering: improved threshold matrices for ordered dithering. In: IEEE international conference on image processing, vol. 2; 1994. p. 1032–5.
[14] Bayer B. An optimum method for two-level rendition of continuous-tone pictures. In: IEEE international conference on communications, vol. 1; 1973. p. 11–5.
[15] Kite TD, Evans BL, Bovik AC. Modeling and quality assessment of Halftoning by error diffusion. In: IEEE international conference on image processing, vol. 9(5); 2000. p. 909–22.
[16] Wang Y, Zhang S. Three-dimensional shape measurement with binary dithered patterns. Appl Opt 2012;51(27):6631–6.
[17] Zhang S. Flexible 3-D shape measurement using projector defocusing: extended measurement range. Opt Lett 2010;35(7):931–3.